Structural Consequences of Electron Hyperdeficiency. Synthesis and Crystal Structure of an Iron–Cobalt Metallocarborane Having Two Closed Polyhedra Fused along an Edge

William M. Maxwell, Ekk Sinn, and Russell N. Grimes*

Contribution from the Department of Chemistry, University of Virginia, Charlottesville, Virginia 22901. *Received September 8, 1975*

Abstract: A metallocarborane of novel structure, $(CH_3)_4C_4B_8H_8FeCo(\eta^5\text{-}C_5H_5)$, has been synthesized and structurally characterized from ^{11}B and ^1H FT NMR, mass spectroscopic, infrared, and single-crystal x-ray diffraction data. The dark green crystals are monoclinic, space group $P2_1$, with two molecules per unit cell and $a = 7.203$ (4) Å, $b = 14.77$ (2) Å, $c = 8.830$ (2) Å, and $\beta = 99.7$ (1)° ($\rho_{calcd} = 1.38$, $\rho_{obsd} = 1.38$ g cm^{-3}). The structure was solved by the heavy-atom method and refined by full-matrix least-squares procedures to a final R value of 0.069 and $R_w = 0.081$ for the 1657 reflections for which $F_o^2 > 3\sigma(F_o)^2$. The molecule contains a direct iron–cobalt bond and consists of two pentagonal bipyramidal units fused at a common iron atom with an additional BH group capping triangular faces on both polyhedra simultaneously. The structure is explained in terms of a shortage of two electrons in the cage framework, relative to the normal requirement for polyhedral clusters, which causes one BH group to adopt a capping location. These results are discussed in relation to the known structures of two osmium carbonyls and a diiron metallocarborane.

Correlations between valence electron population and molecular structure in cluster systems have underlined a fundamental relationship between many diverse kinds of molecules including metal clusters, boron cage species, numerous organometallic compounds, and hydrocarbon cations.[1] For example, the established or postulated structures of the $(CH_3)_6C_6^{2+}$ ion,[2] $(\eta^5\text{-}C_5H_5)_2Fe$ (ferrocene),[3] B_6H_{10},[4] the carborane series $C_nB_{6-n}H_{10-n}$ ($n = 1$-4),[5] and the metallocarborane $(CO)_3FeC_2B_3H_7$[6] all feature a pentagonal pyramidal central framework containing 16 valence electrons exclusive of bonds to ligand atoms (in the case of ferrocene, two such pyramids are fused at the common iron atom). The development of structure-electron counting relationships of this kind into a general, widely applicable approach has given the synthetic chemist a powerful tool for predicting the synthesis, structure, and properties of many new cluster species. A well-tested observation[1] is that a cage framework of n atoms in which the number of electrons available for skeletal bonding (e) is $2n + 2$ will adopt a closed polyhedral geometry in which all faces are triangular; electrons in excess of $2n + 2$ will induce the polyhedron to open or otherwise[1g,7] distort.

Situations in which e is *less than* $2n + 2$ (which we call "electron hyperdeficiency" in recognition of the fact that even the $2n + 2$ systems are electron deficient in the classical sense) are rare, but the few known examples indicate that the geometry is grossly altered in relation to the "normal" $2n + 2$ electron polyhedral case. Thus, the $2n$ electron systems[8] $Os_6(CO)_{18}$ and $Os_7(CO)_{21}$ are respectively a capped trigonal bipyramid and a capped octahedron, in contrast to the octahedral and pentagonal bipyramidal geometry usually encountered in 6- and 7-vertex polyhedra. An apparently similar case arises in the metallocarborane 1,6-$(\eta\text{-}C_5H_5)_2$-1,6,2,3-$Fe_2C_2B_6H_8$,[9] also a $2n$ electron system ($n = 10$), which is not the bicapped square antiprism expected for a 10-vertex system but rather a capped tricapped trigonal prism. All of these observations are accountable on the basis[8,9] that capping a face of a closed polyhedron in at least some cases does not increase the number of bonding orbitals,[10] so that an n-vertex capped polyhedron would accomodate the same number of skeletal bonding electrons ($2n$) as an uncapped polyhedron of $n - 1$ vertices.

In this paper we report the synthesis and structure of a new compound which supports and extends these structural principles in a novel way. The direct-insertion[11] reaction of the metallocarborane $[2,3\text{-}(CH_3)_2C_2B_4H_4]_2FeH_2$[12] with an excess of $(\eta^5\text{-}C_5H_5)Co(CO)_2$ in dry hexane under uv light gave in 11% yield a dark green crystalline air-stable solid formulated as $(CH_3)_4C_4B_8H_8Fe^{II}Co^{III}(\eta^5\text{-}C_5H_5)$. The ^{11}B Fourier transform NMR (FT NMR) spectrum of this compound in $CDCl_3$ exhibited six doublets, partially overlapped, which on proton decoupling collapsed to singlets at δ −92.7, −57.4, −12.4, −8.4, +2.2, and +8.9 ppm relative to boron trifluoride etherate, with relative areas 1:1:3:1:1:1. The proton FT NMR spectrum in $CDCl_3$ contained peaks at τ 5.05 (C_5H_5), 7.97 (CH_3), and 8.08 (CH_3), in an area ratio of 5:3:9. The unit-resolution mass spectrum exhibited a strong high mass cutoff at m/e 384 corresponding to the parent ion, with a pattern of intensities in the parent region consistent with the calculated isotopic composition. Other major groupings having local cutoffs at m/e 282, 270, 124, and 121 corresponded to the $(CH_3)_2C_2B_4H_4FeCo(C_5H_5)^+$, $(CH_3)_2C_2B_3H_3FeCo(C_5H_5)^+$, $Co(C_5H_5)^+$, and $Fe(C_5H_5)^+$ fragments, respectively. The composition was confirmed from the high-resolution chemical ionization mass spectrum in argon–water, which gave a mass of 385.1460 for the protonated (M + 1) species (calcd for $[^{56}Fe^{59}Co^{12}C_{13}{}^{11}B_8{}^1H_{26}]^+$, 385.1459). It was not possible to determine the molecular geometry from the spectroscopic data, but an x-ray crystallographic study established the structure shown in Figure 1.

Experimental Section

Synthesis. A 50-mg quantity of $[2,3\text{-}(CH_3)_2C_2B_4H_4]_2FeH_2$[12] and 300 mg of reagent grade $(\eta^5\text{-}C_5H_5)Co(CO)_2$ were placed in a 5-ml round-bottom flask into which 2 ml of dry hexane was distilled in vacuo. Following irradiation by sun lamp for 23 h, the reaction mixture was opened to the air, stirred, and filtered through a column of silica gel (Merck, 70–230 mesh), washing with dichloromethane. The dichloromethane solution was thick-layer chromatographed on silica gel and developed in cyclohexane. The principal product was a dark greenish brown band (R_f 0.33) of which 8.2 mg was collected.

Spectra. Boron-11 and proton FT NMR spectra at 32.1 and 100 MHz, respectively, were obtained on a JEOL PS-100P pulse Fourier transform instrument. Mass spectra were recorded on Hitachi Perkin-Elmer RMU-6E and AEI MS-902 (double focusing) instruments, the latter equipped with an SRI chemical ionization source. Infrared spectra were recorded on a Beckman IR-8 spectrophotometer.

X-Ray Crystallographic Study. Dark green crystals of

Table I. Positional and Thermal Parameters and Their Estimated Standard Deviations[a]

Atom	X	Y	Z	$B_{1,1}$[b]	$B_{2,2}$	$B_{3,3}$	$B_{1,2}$	$B_{1,3}$	$B_{2,3}$
Co	0.3936 (2)	0.3321 (1)	0.3435 (2)	0.0188 (3)	0.00263 (5)	0.0109 (2)	−0.0010 (3)	−0.0003 (4)	−0.0009 (2)
Fe	0.2027 (2)	0.2651 (1)	0.1105 (2)	0.0187 (3)	0.00183 (5)	0.0101 (2)	0.0007 (3)	−0.0012 (4)	0.0005 (2)
C(4)	0.344 (2)	0.1530 (7)	0.198 (1)	0.028 (3)	0.0021 (4)	0.010 (1)	0.002 (2)	−0.005 (4)	0.001 (1)
CM(4)	0.399 (3)	0.0619 (8)	0.135 (2)	0.055 (5)	0.0029 (5)	0.016 (2)	0.017 (3)	0.001 (6)	−0.000 (2)
C(5)	0.177 (2)	0.1642 (7)	0.266 (1)	0.028 (3)	0.0021 (4)	0.011 (2)	−0.004 (2)	−0.005 (4)	0.002 (1)
CM(5)	0.035 (3)	0.0891 (10)	0.282 (2)	0.046 (5)	0.0046 (6)	0.018 (2)	−0.017 (3)	−0.001 (6)	0.002 (2)
C(4′)	0.171(2)	0.2378 (7)	−0.123 (1)	0.00 (3)	0.0027 (5)	0.007 (1)	0.002 (2)	−0.002 (4)	0.001 (1)
CM(4′)	0.214 (3)	0.1590 (10)	−0.223 (1)	0.048 (5)	0.0055 (7)	0.011 (2)	0.009 (4)	0.005 (5)	−0.004 (2)
C(5′)	−0.013 (2)	0.2483 (6)	−0.078 (1)	0.023 (3)	0.0016 (5)	0.010 (1)	0.000 (2)	0.001 (3)	0.001 (1)
CM(5′)	−0.176 (2)	0.1825 (10)	−0.126 (2)	0.036 (4)	0.0046 (7)	0.020 (2)	−0.011 (3)	−0.005 (6)	−0.002 (2)
C(11)	0.430 (2)	0.4736 (9)	0.360 (2)	0.046 (5)	0.0024 (5)	0.031 (3)	−0.005 (3)	−0.036 (6)	−0.006 (2)
C(12)	0.592 (2)	0.4350 (10)	0.329 (2)	0.042 (4)	0.0053 (7)	0.024 (3)	−0.019 (3)	−0.002 (6)	−0.002 (2)
C(13)	0.660 (2)	0.3720 (10)	0.447 (2)	0.023 (3)	0.0056 (7)	0.034 (3)	−0.002 (3)	−0.016 (6)	−0.012 (3)
C(14)	0.546 (2)	0.3741 (10)	0.554 (1)	0.032 (4)	0.0069 (8)	0.012 (2)	−0.009 (3)	−0.001 (4)	−0.007 (2)
C(15)	0.402 (2)	0.4353 (10)	0.509 (2)	0.035 (4)	0.0080 (8)	0.025 (2)	−0.011 (3)	0.016 (5)	−0.020 (2)
B(3)	0.478 (2)	0.2400 (11)	0.215 (1)	0.028 (4)	0.0058 (8)	0.008 (2)	0.008 (3)	−0.000 (4)	0.003 (2)
B(6)	0.164 (2)	0.2617 (11)	0.343 (1)	0.017 (3)	0.0038 (6)	0.011 (2)	0.000 (3)	0.003 (3)	−0.000 (2)
B(7)	0.381 (2)	0.1992 (11)	0.381 (2)	0.031 (4)	0.0043 (7)	0.010 (2)	0.002 (3)	−0.004 (5)	0.001 (2)
B(8)	0.133 (2)	0.3661 (9)	0.224 (2)	0.022 (3)	0.0024 (5)	0.013 (2)	0.003 (2)	−0.003 (4)	0.001 (2)
B(2′)	0.171 (2)	0.3959 (10)	−0.001 (1)	0.029 (4)	0.0030 (6)	0.011 (2)	−0.000 (3)	−0.008 (5)	0.001 (2)
B(3′)	0.304 (2)	0.3186 (10)	−0.078 (2)	0.021 (3)	0.0045 (7)	0.011 (2)	0.001 (3)	−0.002 (4)	0.002 (2)
B(6′)	−0.037 (2)	0.3441 (10)	−0.003 (2)	0.022 (3)	0.0034 (6)	0.018 (2)	0.006 (3)	0.002 (5)	0.000 (2)
B(7′)	0.065 (2)	0.3430 (10)	−0.168 (1)	0.034 (4)	0.0035 (6)	0.011 (2)	0.000 (3)	−0.015 (5)	0.007 (2)
H(3)	0.5945	0.2474	0.623	5.0					
H(6)	0.0563	0.2706	0.3983	5.0					
H(7)	0.4480 (0)	0.1760 (0)	0.4840 (0)	5.0					
H(8)	0.0558 (0)	0.4207 (0)	0.1954 (0)	5.0					
H(11)	0.3447 (0)	0.5207 (0)	0.3107 (0)	5.0					
H(12)	0.6479 (0)	0.4500 (0)	0.2360 (0)	5.0					
H(13)	0.7710 (0)	0.3335 (0)	0.4520 (0)	5.0					
H(14)	0.5593 (0)	0.3383 (0)	0.6488 (0)	5.0					
H(15)	0.3005 (0)	0.4518 (0)	0.5671 (0)	5.0					
H(2′)	0.2068 (0)	0.4598 (0)	0.0349 (0)	5.0					
H(3′)	0.4401 (0)	0.3254 (0)	−0.0914 (0)	5.0					
H(6′)	−0.1489 (0)	0.3689 (0)	0.0388 (0)	5.0					
H(7′)	0.0139 (0)	0.3718 (0)	−0.2722 (0)	5.0					

[a] The form of the anisotropic thermal parameter is: $\exp[-(B_{1,1}hh + B_{2,2}kk + B_{3,3}ll + B_{1,2}hk + B_{1,3}hl + B_{2,3}kl)]$. [b] B (Å^2) for the H atoms.

Table II. Bond Distances (Å)

Fe-Co	2.480 (1)	C(5′)-C(4′)	1.453 (8)
Fe-C(5′)	2.093 (5)	C(5′)-B(7′)	1.745 (9)
Fe-C(4′)	2.074 (5)	C(5′)-B(6′)	1.588 (9)
Fe-C(4)	2.029 (5)	C(4′)-CM(4′)	1.522 (8)
Fe-C(5)	2.059 (6)	C(4′)-B(7′)	1.749 (9)
Fe-B(6′)	2.183 (7)	C(4′)-B(3′)	1.537 (9)
Fe-B(2′)	2.164 (7)	C(4)-CM(4)	1.533 (8)
Fe-B(3′)	2.080 (7)	C(4)-C(5)	1.447 (9)
Fe-B(6)	2.122 (6)	C(4)-B(7)	1.732 (9)
Fe-B(8)	1.912 (7)	C(4)-B(3)	1.59 (1)
Fe-B(3)	2.072 (8)	C(5)-CM(5)	1.529 (9)
Co-C(11)	2.112 (7)	C(5)-B(6)	1.602 (9)
Co-C(12)	2.104 (7)	C(5)-B(7)	1.72 (1)
Co-C(13)	2.067 (7)	B(7′)-B(6′)	1.74 (1)
Co-C(14)	2.084 (6)	B(7′)-B(2′)	1.726 (9)
Co-C(15)	2.105 (7)	B(7′)-B(3′)	1.81 (1)
Co-B(6)	1.953 (7)	B(6′)-B(2′)	1.68 (1)
Co-B(8)	2.057 (7)	B(6′)-B(8)	2.19 (1)
Co-B(7)	1.997 (8)	B(2′)-B(3′)	1.70 (1)
Co-B(3)	1.935 (7)	B(2′)-B(8)	2.10 (1)
C(11)-C(12)	1.40 (1)	B(6)-B(8)	1.86 (1)
C(11)-C(15)	1.41 (1)	B(6)-B(7)	1.80 (1)
C(12)-C(13)	1.42 (1)	B(7)-B(3)	1.83 (1)
C(13)-C(14)	1.35 (1)	C(5′)-CM(5′)	1.531 (9)
C(14)-C(15)	1.38 (1)		

$(CH_3)_4C_4B_8H_8FeCo(\eta^5\text{-}C_5H_5)$ were grown by slow evaporation of a hexane–dichloromethane solution, and the crystal density was measured by flotation in aqueous KI solution. Crystal data: $FeC_{13}B_8H_{25}$; M = 384; space group $P2_1$, $Z = 2$; $a = 7.203$ (4), $b = 14.77$ (2), $c = 8.830$ (2) Å; $\beta = 99.7$ (1)°; $V = 925$ Å^3; μ(Mo Kα) = 17.3 cm^{-1}; $\rho_c = 1.38$, $\rho_o = 1.38$ (2) g cm^{-3}; $F(000) = 382$. For the chosen crystal, the Enraf-Nonius program SEARCH was used to obtain 15 accurately centered reflections which were then used in the program INDEX to obtain an orientation matrix for data collection and also to provide approximate cell dimensions. Refined cell dimensions

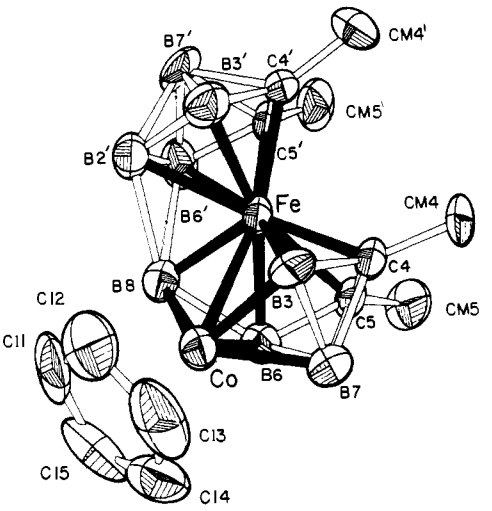

Figure 1. Molecular structure and numbering system for $(CH_3)_4C_4B_8H_8FeCo(\eta^5\text{-}C_5H_5)$. Hydrogen atoms are excluded for clarity.

Table III. Bond Angles (deg)

Co-Fe-C(5′)	160.3 (1)	C(4′)-Fe-B(3)	110.0 (3)	C(12)-C(13)-C(14)	108.7 (8)	CM(4)-C(4)-C(5)	122.3 (6)
Co-Fe-C(4′)	148.6 (2)	C(4)-Fe-C(5)	41.5 (3)	Co-C(14)-C(13)	70.3 (4)	CM(4)-C(4)-B(7)	132.6 (5)
Co-Fe-C(4)	80.5 (2)	C(4)-Fe-B(6′)	156.9 (3)	Co-C(14)-C(15)	71.5 (4)	CM(4)-C(4)-B(3)	123.5 (6)
Co-Fe-C(5)	80.5 (2)	C(4)-Fe-B(2′)	155.6 (3)	C(13)-C(14)-C(15)	109.4 (8)	C(5)-C(4)-B(7)	64.9 (4)
Co-Fe-B(6′)	116.8 (2)	C(4)-Fe-B(3′)	113.3 (3)	Co-C(15)-C(14)	69.9 (4)	C(5)-C(4)-B(3)	113.8 (5)
Co-Fe-B(2′)	91.3 (2)	C(4)-Fe-B(6)	75.5 (3)	Co-C(15)-C(11)	70.7 (4)	B(7)-C(4)-B(3)	66.7 (4)
Co-Fe-B(3′)	107.0 (2)	C(4)-Fe-B(8)	126.6 (3)	C(11)-C(15)-C(14)	107.5 (8)	Fe-C(5)-C(4)	68.2 (3)
Co-Fe-B(6)	49.5 (2)	C(4)-Fe-B(3)	45.8 (3)	Fe-C(5′)-C(4′)	68.9 (3)	Fe-C(5)-CM(5)	136.4 (5)
Co-Fe-B(8)	54.0 (2)	C(5)-Fe-B(6′)	122.6 (3)	Fe-C(5′)-B(7′)	90.8 (3)	Fe-C(5)-B(6)	69.6 (3)
Co-Fe-B(3)	49.3 (2)	C(5)-Fe-B(2′)	159.5 (3)	Fe-C(5′)-B(6′)	71.3 (3)	Fe-C(5)-B(7)	90.7 (4)
C(5′)-Fe-C(4′)	40.8 (2)	C(5)-Fe-B(3′)	153.3 (3)	C(4′)-C(5′)-B(7′)	65.5 (4)	C(4)-C(5)-CM(5)	124.9 (6)
C(5′)-Fe-C(4)	117.8 (2)	C(5)-Fe-B(6)	45.0 (3)	C(4′)-C(5′)-B(6′)	112.3 (5)	C(4)-C(5)-B(6)	112.9 (5)
C(5′)-Fe-C(5)	108.0 (2)	C(5)-Fe-B(8)	98.8 (3)	B(7′)-C(5′)-B(6′)	62.8 (4)	C(4)-C(5)-B(7)	65.6 (5)
C(5′)-Fe-B(6′)	43.6 (2)	C(5)-Fe-B(3)	76.2 (3)	Fe-C(4′)-C(5′)	70.3 (3)	CM(5)-C(5)-B(6)	121.8 (6)
C(5′)-Fe-B(2′)	74.6 (2)	B(6′)-Fe-B(2′)	45.5 (3)	Fe-C(4′)-CM(4′)	136.5 (4)	CM(5)-C(5)-B(7)	132.9 (5)
C(5′)-Fe-B(3′)	73.7 (2)	B(6′)-Fe-B(3′)	77.7 (3)	Fe-C(4′)-B(7′)	91.4 (3)	B(6)-C(5)-B(7)	65.4 (4)
C(5′)-Fe-B(6)	124.7 (2)	B(6′)-Fe-B(6)	103.5 (3)	Fe-C(4′)-B(3′)	68.5 (3)	C(5′)-B(7′)-C(4′)	49.2 (3)
C(5′)-Fe-B(8)	106.5 (3)	B(6′)-Fe-B(8)	64.1 (3)	C(5′)-C(4′)-CM(4′)	121.3 (6)	C(5′)-B(7′)-B(6′)	54.2 (4)
C(5′)-Fe-B(3)	149.1 (3)	B(6′)-Fe-B(3)	157.3 (3)	C(5′)-C(4′)-B(7′)	65.3 (4)	C(5′)-B(7′)-B(2′)	96.1 (4)
C(4′)-Fe-C(4)	100.7 (2)	B(2′)-Fe-B(3′)	47.2 (3)	C(5′)-C(4′)-B(3′)	113.7 (5)	C(5′)-B(7′)-B(3′)	89.7 (4)
C(4′)-Fe-C(5)	121.1 (2)	B(2′)-Fe-B(6)	116.2 (3)	CM(4′)-C(4′)-B(7′)	132.1 (4)	C(4′)-B(7′)-B(6′)	92.8 (4)
C(4′)-Fe-B(6′)	72.8 (3)	B(2′)-Fe-B(8)	61.6 (3)	CM(4′)-C(4′)-B(3′)	124.7 (6)	C(4′)-B(7′)-B(2′)	95.4 (4)
C(4′)-Fe-B(2′)	74.6 (2)	B(2′)-Fe-B(3)	112.5 (3)	B(7′)-C(4′)-B(3′)	66.3 (4)	C(4′)-B(7′)-B(3′)	51.2 (4)
C(4′)-Fe-B(3′)	43.4 (2)	B(3′)-Fe-B(6)	154.7 (3)	Fe-C(4)-CM(4)	136.1 (4)	B(6′)-B(7′)-B(2′)	58.0 (4)
C(4′)-Fe-B(6)	161.5 (2)	B(3′)-Fe-B(8)	106.3 (3)	Fe-C(4)-C(5)	70.4 (3)	B(6′)-B(7′)-B(3′)	97.9 (4)
C(4′)-Fe-B(8)	132.7 (3)	B(3′)-Fe-B(3)	89.2 (3)	B(2′)-B(7′)-B(3′)	57.5 (4)	Fe-B(6)-C(5)	65.4 (3)
B(6)-Fe-B(8)	54.6 (3)	C(13)-Co-C(14)	38.0 (3)	Fe-B(6′)-C(5′)	65.2 (3)	Fe-B(6)-B(7)	86.6 (3)
B(6)-Fe-B(3)	80.6 (3)	C(13)-Co-C(15)	64.7 (3)	Fe-B(6′)-B(7′)	87.9 (4)	Co-B(6)-C(5)	111.7 (4)
B(8)-Fe-B(3)	102.9 (3)	C(13)-Co-B(6)	151.0 (4)	Fe-B(6′)-B(2′)	66.7 (3)	Co-B(6)-B(7)	64.1 (3)
Fe-Co-C(11)	121.5 (2)	C(13)-Co-B(8)	149.0 (3)	Fe-B(6′)-B(8)	51.9 (3)	C(5)-B(6)-B(7)	60.5 (4)
Fe-Co-C(12)	121.7 (2)	C(13)-Co-B(7)	105.7 (4)	C(5′)-B(6′)-B(7′)	63.0 (4)	Fe-B(8)-Co	77.2 (3)
Fe-Co-C(13)	145.5 (3)	C(13)-Co-B(3)	95.8 (3)	C(5′)-B(6′)-B(2′)	104.2 (5)	Fe-B(8)-B(6′)	63.9 (3)
Fe-Co-C(14)	172.9 (2)	C(14)-Co-C(15)	38.6 (3)	C(5′)-B(6′)-B(8)	115.7 (5)	Fe-B(8)-B(2′)	65.1 (3)
Fe-Co-C(15)	144.2 (3)	C(14)-Co-B(6)	118.5 (3)	B(7′)-B(6′)-B(2′)	60.5 (4)	Co-B(8)-B(6′)	139.1 (4)
Fe-Co-B(6)	55.7 (2)	C(14)-Co-B(8)	133.1 (4)	B(7′)-B(6′)-B(8)	121.2 (5)	Co-B(8)-B(2′)	106.4 (4)
Fe-Co-B(8)	48.8 (2)	C(14)-Co-B(7)	100.1 (3)	B(2′)-B(6′)-B(8)	64.2 (4)	B(6′)-B(8)-B(2′)	46.2 (3)
Fe-Co-B(7)	73.3 (2)	C(14)-Co-B(3)	124.2 (4)	Fe-B(2′)-B(7′)	89.0 (4)	Co-B(7)-C(4)	103.6 (4)
Fe-Co-B(3)	54.3 (2)	C(15)-Co-B(6)	108.0 (3)	Fe-B(2′)-B(6′)	67.8 (3)	Co-B(7)-C(5)	104.7 (4)
C(11)-Co-C(12)	38.7 (3)	C(15)-Co-B(8)	95.5 (4)	Fe-B(2′)-B(3′)	63.8 (3)	Co-B(7)-B(6)	61.7 (4)
C(11)-Co-C(13)	65.4 (3)	C(15)-Co-B(7)	126.3 (4)	Fe-B(2′)-B(8)	53.3 (3)	Co-B(7)-B(3)	60.5 (4)
C(11)-Co-C(14)	64.9 (3)	C(15)-Co-B(3)	160.4 (3)	B(7′)-B(2′)-B(6′)	61.5 (4)	C(4)-B(7)-C(5)	49.5 (4)
C(11)-Co-C(15)	39.1 (3)	B(6)-Co-B(8)	55.2 (3)	B(7′)-B(2′)-B(3′)	63.6 (4)	C(4)-B(7)-B(6)	92.1 (5)
C(11)-Co-B(6)	128.0 (4)	B(6)-Co-B(7)	54.2 (3)	B(7′)-B(2′)-B(8)	127.1 (5)	C(4)-B(7)-B(3)	53.1 (4)
C(11)-Co-B(8)	84.1 (3)	B(6)-Co-B(3)	88.5 (3)	B(6′)-B(2′)-B(3′)	104.6 (5)	C(5)-B(7)-B(6)	54.1 (4)
C(11)-Co-B(7)	164.5 (3)	B(8)-Co-B(7)	105.3 (3)	B(6′)-B(2′)-B(8)	69.6 (4)	C(5)-B(7)-B(3)	91.6 (5)
C(11)-Co-B(3)	135.3 (5)	B(8)-Co-B(3)	102.7 (3)	B(3′)-B(2′)-B(8)	114.1 (5)	B(6)-B(7)-B(3)	96.7 (5)
C(12)-Co-C(13)	39.8 (3)	B(7)-Co-B(3)	55.5 (3)	Fe-B(3′)-C(4′)	68.1 (3)	Fe-B(3)-Co	76.4 (3)
C(12)-Co-C(14)	65.1 (3)	Co-C(11)-c)12)	70.4 (4)	Fe-B(3′)-B(7′)	89.6 (4)	Fe-B(3)-C(4)	65.7 (4)
C(12)-Co-C(15)	65.2 (3)	Co-C(11)-C(15)	70.2 (5)	OFe-B(3′)-B(2′)	69.0 (3)	Fe-B(3)-B(7)	87.3 (4)
C(12)-Co-B(6)	165.5 (4)	C(12)-C(11)-C(15)	107.8 (8)	C(4′)-B(3′)-B(7′)	62.5 (4)	Co-B(3)-C(4)	112.1 (5)
C(12)-Co-B(8)	111.3 (4)	Co-C(12)-C(11)	71.0 (5)	C(4′)-B(3′)-B(2′)	105.0 (5)	Co-B(3)-B(7)	63.9 (4)
C(12)-Co-B(7)	140.4 (4)	Co-C(12)-C(13)	68.7 (4)	B(7′)-B(3′)-B(2′)	58.9 (4)	C(4)-B(3)-B(7)	60.3 (4)
C(12)-Co-B(3)	100.9 (4)	C(11)-C(12)-C(13)	106.6 (8)	Fe-B(6)-Co	74.8 (2)	CM(5′)-C(5′)-Fe	136.7 (5)
Co-C(13)-C(12)	71.5 (4)	Fe-C(4)-B(7)	91.4 (4)	CM(5′)-C(5′)-C(4′)	123.7 (5)		
Co-C(13)-C(14)	71.7 (4)	Fe-C(4)-B(3)	68.5 (3)	CM(5′)-C(5′)-B(7′)	132.4 (6)		
				CM(5′)-C(5′)-B(6′)	123.1 (5)		

and their estimated standard deviations were obtained from least-squares refinement of 28 accurately centered reflections. The mosaicity of the crystal was examined by the ω scan technique and found marginally acceptable. The choice of the acentric space group as an initial working assumption was based on the known empirical formula, assuming an approximate volume of 19 Å^3 per non-hydrogen atom. This hypothesis was ultimately confirmed by the solution of the structure. In fact, parallel calculations were performed for a center of symmetry in the early stages of refinement and produced consistently higher R values.

Collection and Reduction of the Data. Diffraction data were collected at 292 K on an Enraf-Nonius four-circle CAD-4 diffractometer controlled by a PDP8/M computer, using Mo Kα radiation from a highly oriented graphite crystal monochromator. The θ-2θ scan technique was used to record the intensities for all reflections for which $1° < 2\theta < 52°$. Scan widths (SW) were calculated from the formula SW = $A + B \tan\theta$, where A is estimated from the mosaicity of the crystal and B allows for the increase in width of peak due to Kα_1 and Kα_2 splitting. The values of A and B were 0.6 and 0.2°, respectively. This calculated scan angle was extended at each side by 25% for background determination (BG1 and BG2). The net count (NC) was then calculated as NC = TOT − 2(BG1 + BG2) where TOT is the estimated peak intensity. Reflection data were considered insignificant if intensities registered less than ten counts above background on a rapid prescan, such reflections being rejected automatically by the computer. The intensities of four standard reflections, monitored for each crystal at 100 reflection intervals, showed no greater fluctuations during the data collection than those expected from Poisson statistics. The raw intensity data were collected for Lorentz-polarization effects, and then for absorption, applying spherical absorption corrections. After averaging the intensities of equivalent reflections, (hkl and $\bar{h}\bar{k}\bar{l}$), the data were reduced to 1731 intensities of which 1657 had $F_o^2 >$

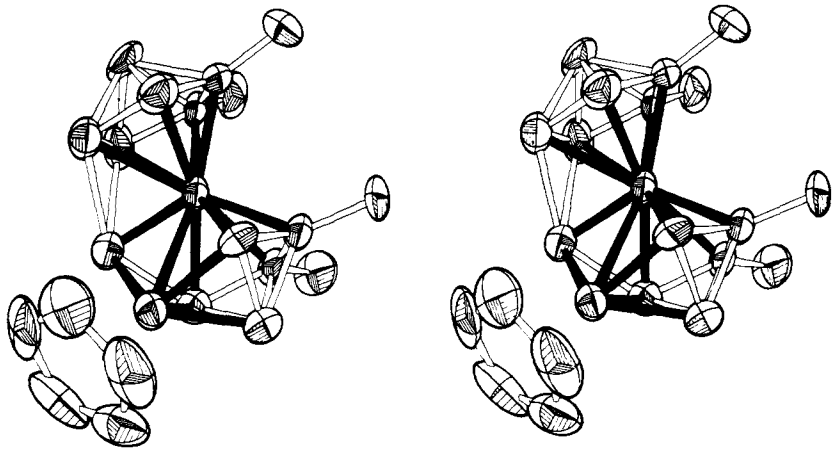

Figure 2. Stereoscopic pair view of the molecule, excluding hydrogen atoms.

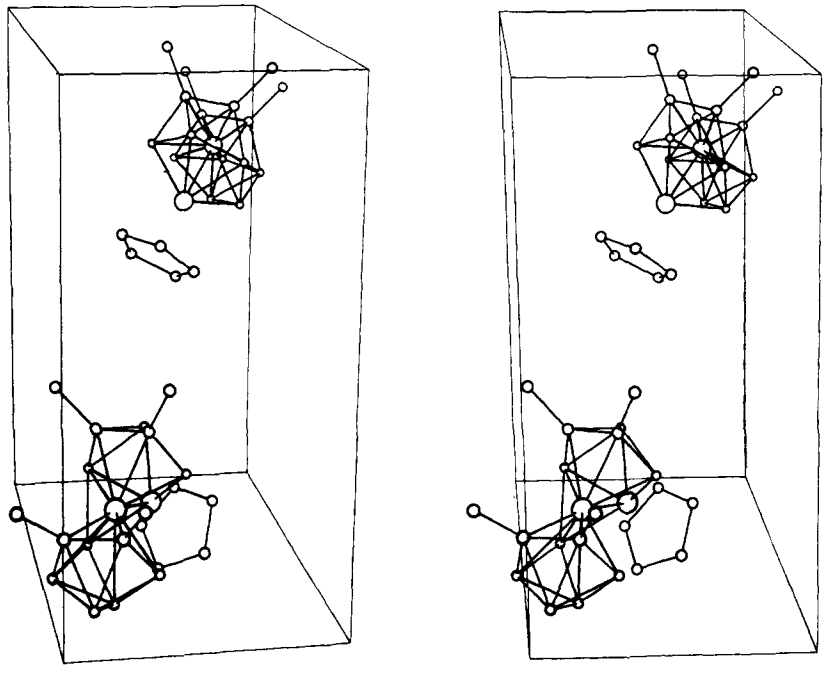

Figure 3. Stereoscopic view of the molecular packing in the unit cell.

$3\sigma(F_o)^2$, where $\sigma(F_o)^2$ was estimated from counting statistics.[13] These data were used in the final refinement of the structural parameters.

Solution and Refinement of the Structure. The coordinates of the two heavy atoms were determined from a three-dimensional Patterson synthesis. Full-matrix least-squares refinement was based on F, and the function was minimized as $\Sigma w(|F_o| - |F_c|)^2$. The weights w were taken as $[2F_o/\sigma(F_o^2)]^2$ where $|F_o|$ and $|F_c|$ are the observed and calculated structure factor amplitudes. The atomic scattering factors for non-hydrogen atoms were taken from Cromer and Waber[14] and those for hydrogen from Stewart.[15] The effects of anomalous dispersion were included in F_c using Cromer and Ibers[16] values for $\Delta f'$ and $\Delta f''$. Agreement factors are defined as $R = \Sigma||F_o| - |F_c||/\Sigma|F_o|$ and $R_w = (\Sigma w(|F_o| - |F_c|)^2/\Sigma w|F_o|^2)^{1/2}$. In order to minimize computer time, the initial calculations were carried out on the first 900 reflections collected. The computing system and programs used are described elsewhere.[17] The intensity data were phased sufficiently well by the metal positions to permit location of the remaining non-hydrogen atoms by difference Fourier syntheses, the cage carbon atoms being identified by the positions of their methyl substituents. After full-matrix least-squares refinement the model converged with $R = 10.0\%$.

The arrangement of boron atoms was recognized as unusual. Consequently, after adding the remaining reflection data to the calculation, a difference Fourier synthesis was calculated using all non-hydrogen, non-boron atoms to phase the data. This located the same boron positions and also gave the first indication of hydrogen atom locations. Anisotropic temperature factors were introduced for all non-hydrogen atoms, and non-methyl hydrogen atoms except for H(8) were introduced as fixed atoms at the calculated positions with isotropic temperature factors of 5.0 Å^2, assuming a B(C)-H distance of 1.0 Å. Atom H(8) was now located on a difference Fourier map, refined for one cycle of least-squares refinement together with the non-hydrogen atoms, and thereafter held fixed. After convergence, all other non-methyl hydrogen atoms were inserted at their new calculated positions. The model converged with $R = 6.9\%$, $R_w = 8.1\%$, which in view of the relatively poor crystal quality was considered good.

Interchange of the Co and Fe positions produced an improbable imbalance in the temperature factors and a rise of 0.1% in R. While this does not constitute an unambiguous test for the metal positions, their assigned locations are supported beyond reasonable doubt by the method of synthesis. The absolute configuration was determined by calculation of F_c's for both possible configurations[18] and comparison with F_o, for the two models; the enantiomorph of the configuration in Figure 1 can just be rejected at the 5% level of significance.[19] The effect is small because the $\Delta f''$ values are small with Mo Kα radiation. Since y is arbitrary in $P2_1$, the y coordinate of Fe was set at 0.25 and treated as a fixed parameter for most of the calculations. This parameter became unfixed after a power failure near the end of refinement, but it was deemed unwarranted in terms of computer time to reset this parameter to 0.25 (corresponding to a small translation

Table IV. Closest Intermolecular Contacts (Å)

Molecule 1	Molecule 2	Distance	Symmetry operation		
C12	CM4′	3.78	$1-x$	$\frac{1}{2}+y$	$-z$
C15	CM4	3.72	$1-x$	$\frac{1}{2}+y$	$1-z$
CM4′	C4	3.78	$1-x$	$y-\frac{1}{2}$	$1-z$
CM5	B7	3.81	$-x$	$y-\frac{1}{2}$	$-z$

of the entire structure along b).

The error in an observation of unit weight is 5.1. A structure factor calculation with all observed and unobserved reflections included (without refinement) gave $R = 7.1\%$; on this basis it was decided that careful measurement of reflections rejected automatically during data collection would not significantly improve the results. A final Fourier difference map was featureless. A table of the observed structure factors is available.[20]

Discussion

Final positional and thermal parameters for the compound are given in Table I, while Tables II and III contain the bond lengths and angles. The digits in parentheses in the tables are the estimated standard deviations in the least significant figures quoted, and were derived from the inverse matrix in the course of least-squares refinement calculations. The molecular structure and numbering are given in Figure 1, Figure 2 is a stereoscopic pair view of the complex, and Figure 3 depicts the molecular packing in the unit cell. As is evident from the packing diagram and the closest intermolecular distances (Table IV), the complex molecules are well separated with no particularly close contacts. Table V presents information on relevant mean planes and interplanar angles within the molecule.

The direct iron-cobalt bond is the first such feature to be measured in a boron cage and has a length of 2.480 (1) Å which may be compared with known cobalt-cobalt distances of 2.444 (2),[21] 2.489 (1),[22] and 2.387 (2) Å[23] in the structures of 1,7,5,6-$(\eta^5\text{-}C_5H_5)_2Co_2C_2B_5H_7$, 2,6,1,10-$(\eta^5\text{-}C_5H_5)_2Co_2C_2B_6H_8$, and 2,3,1,7-$(\eta^5\text{-}C_5H_5)_2Co_2C_2B_8H_{10}$, respectively. It should be noted that each of these metal-metal bonded metallocarboranes incorporates a different polyhedral geometry, and the effect of cage geometry on the bond lengths quoted is something of an unknown factor at present. However, all of these metal-metal interactions are within or shorter than the range of Co-Co bond distances (2.43-2.55 Å) in cobalt clusters such as $(CO)_9Co_3H$.[24,25]

The particularly significant feature of this structure is the unique boron atom B(8) which is wedged between two pentagonal bipyramidal cages defined respectively by Fe, Co, B(3), C(4), C(5), B(6), B(7), and by Fe, B(2′), B(3′), C(4′), C(5′), B(6′), B(7′). Atom B(8) is located 1.912 (7) Å from Fe, 2.057 (7) from Co, 1.86 (1) from B(6), 2.10 (1) from B(2′), and 2.19 (1) from B(6′). All other bond lengths (Table II) are within normal bond lengths for metallocarboranes. While the B(8)-B(2′) and B(8)-B(6′) distances are relatively long, comparison with other metallocarborane B-B lengths[26] suggests that B(8) is significantly bonded to B(2′) and B(6′). In effect, the B(8)-H unit can be viewed as capping the Fe-Co-B(6) and Fe-B(2′)-B(6′) faces of the two pentagonal bipyramids simultaneously, with slightly stronger interaction with respect to the Fe-Co-B(6) face.

A view of the bonding based on the skeletal electron-counting approach[1] is as follows. Insertion of a $(\eta^5\text{-}C_5H_5)Co$ unit (a two-electron donor) into the $[(CH_3)_2C_2B_4H_4]_2FeH_2$ precursor, with concomitant loss of the two "extra" hydrogens, increases the number of framework atoms (n) without increasing the number of framework electrons. Thus, whereas the precursor contains $2n + 2$ electrons in each of its two 7-vertex polyhedra, the product $(CH_3)_4C_4B_8H_8FeCo(\eta^5\text{-}C_5H_5)$ has two electrons fewer than the number required for the "normal" geometry, which would consist of a 7-vertex pentagonal bipyramidal FeC_2B_4 cage fused at the iron atom to an 8-vertex dodecahedral (distorted square antiprism) $FeCoC_2B_4$ polyhedron. Compensation for this electron shortage is achieved, as in the $2n$ electron systems mentioned earlier, by shifting one BH group to a capping position, except that in the present case the capping atom interacts with faces on both polyhedra. This "double capping" avoids the 3-coordination at the B(8)-H vertex which would occur if only one of the cages were capped. The effect is that of two polyhedra (capped pentagonal bipyramids) sharing an edge. We know of no precedents either for capped pentagonal bipyramids[28] or for closed polyhedra of any type fused on a common edge.

Table V. Selected Molecular Planes

Atom	Deviation, Å	Atom[a]	Deviation, Å
Plane 1: Cyclopentadienyl Ring $0.4803x + 0.7231y + 0.4965z = 7.8740$			
C11	0.002	C14	−0.005
C12	−0.005	C15	0.002
C13	0.007	*Co	1.727
Plane 2: Pentagonal Bipyramid Equator (C_2B_3) $-0.1804x + 0.3909y - 0.9026z = 2.0585$			
B2′	0.015	C5′	−0.013
B3′	−0.023	B6′	−0.003
c4′	−0.024	*Fe	−1.629
Plane 3: Pentagonal Bipyramid Equator (CoC_2B_2) $-0.3331x + 0.4101y - 0.8490z = -1.2361$			
Co	−0.064	C5	−0.029
B3	0.063	B6	0.061
OV4	−0.031	*Fe	1.594
Plane 4: Co, B6, B8 $-0.3283x + 0.5209y + 0.7880z = 4.1489$			
Plane 5: B2′, B6′, B8 $-0.4548x + 0.8888y + 0.0575z = 4.6359$			

Planes	Dihedral angle, deg	Planes	Dihedral angle, deg
2,3	9.35	3,4	69.76
2,4	63.36	3,5	117.85
2,5	112.18	4,5	48.88

[a] Atoms marked with an asterisk are not included in the calculated plane.

The addition or withdrawal of electrons to or from $(CH_3)_4C_4B_8H_8FeCo(\eta^5\text{-}C_5H_5)$ (e.g., by replacing one or both metal atoms with different metals) should effect further structural changes in accordance with the principles discussed above. For example, reduction in the framework electron population may induce additional boron atoms to move into capping or bicapping locations, thereby approaching a situation in which the central metal atom is enclosed within a carborane cage. In the opposite direction, *addition* of two electrons, as in the unknown species $(CH_3)_4C_4B_8H_8NiCo(\eta^5\text{-}C_5H_5)$, should produce a shift to "normal" polyhedral geometry consisting of fused 7- and 8-vertex polyhedra with $2n + 2$ electrons in each cage. In our current synthetic and structural investigations we are attempting to test these hypotheses.

Acknowledgments. We are grateful to Dr. Vernon Miller for helpful discussions, and to the Office of Naval Research for support of this work. The Fourier transform NMR and x-ray crystallographic data were collected on instrumentation acquired in part through grants to the Department of Chemistry from the National Science Foundation.

Supplementary Material Available: A listing of observed structure factors (11 pages). Ordering information is given on any current masthead page.

References and Notes

(1) (a) A recent review in this area is given by K. Wade, *Chem. Brit.*, **11**, 177 (1975). See also (b) K. Wade, *J. Chem. Soc. D*, 792 (1971); (c) K. Wade, *Inorg. Nucl. Chem. Lett.*, **8**, 559, 563, and 823 (1972); (d) R. W. Rudolph and W. R. Pretzer, *Inorg. Chem.*, **11**, 1974 (1972); (e) D. M. P. Mingos, *Nature (London) Phys. Sci.*, **236**, 99 (1972); (f) C. J. Jones, W. J. Evans, and M. F. Hawthorne, *J. Chem. Soc., Chem. Commun.*, 543 (1973); (g) R. N. Grimes, *Ann. N.Y. Acad. Sci.*, **239**, 180 (1974).
(2) H. Hogoveen and P. W. Kwant, *J. Am. Chem. Soc.*, **96**, 2208 (1974).
(3) (a) E. A. Seibold and L. E. Sutton, *J. Chem. Phys.*, **23**, 1966 (1955); (b) J. D. Dunitz, L. E. Orgel, and A. Rich, *Acta Crystallogr.*, **9**, 373 (1956).
(4) F. L. Hirshfeld, K. Eriks, R. E. Dickerson, E. L. Lippert, Jr., and W. N. Lipscomb, *J. Chem. Phys.*, **28**, 56 (1958).
(5) R. N. Grimes, "Carboranes", Academic Press, New York, N.Y., 1970.
(6) J. P. Brennan, R. N. Grimes, R. Schaeffer, and L. G. Sneddon, *Inorg. Chem.*, **12**, 2266 (1973).
(7) R. N. Grimes, *Pure Appl. Chem.*, **39**, 455 (1974).
(8) R. Mason, K. M. Thomas, and D. M. P. Mingos, *J. Am. Chem. Soc.*, **95**, 3802 (1973).
(9) K. P. Callahan, W. J. Evans, F. Y. Lo, C. E. Strouse, and M. F. Hawthorne, *J. Am. Chem. Soc.*, **97**, 296 (1975).
(10) R. Hoffman and W. N. Lipscomb, *J. Chem. Phys.*, **36**, 2179 (1962).
(11) V. R. Miller, L. G. Sneddon, D. C. Beer, and R. N. Grimes, *J. Am. Chem. Soc.*, **96**, 3090 (1974).
(12) (a) W. M. Maxwell, V. R. Miller, and R. N. Grimes, *J. Am. Chem. Soc.*, **96**, 7116 (1974); (b) W. M. Maxwell, V. R. Miller, and R. N. Grimes, *Inorg. Chem.*, in press.
(13) P. W. R. Corfield, R. J. Doedens, and J. A. Ibers, *Inorg. Chem.*, **6**, 197 (1967).
(14) D. T. Cromer and J. T. Waber, "International Tables for X-Ray Crystallography", Vol. IV, The Kynoch Press, Birmingham, England, 1974.
(15) R. F. Stewart, E. R. Davidson, and W. T. Simpson, *J. Chem. Phys.*, **42**, 3175 (1965).
(16) D. T. Cromer and J. A. Ibers, ref 14.
(17) D. P. Freyberg, G. M. Mockler, and E. Sinn, *J. Chem. Soc., Dalton Trans.*, in press.
(18) J. A. Ibers and W. C. Hamilton, *Acta Crystallogr.*, **17**, 781 (1964).
(19) W. C. Hamilton, *Acta Crystallogr.*, **18**, 502 (1965).
(20) See paragraph at end of paper regarding supplementary material.
(21) R. N. Grimes, A. Zalkin, and W. T. Robinson, submitted for publication.
(22) E. L. Hoel, C. E. Strouse, and M. F. Hawthorne, *Inorg. Chem.*, **13**, 1388 (1974).
(23) K. P. Callahan, C. E. Strouse, A. L. Sims, and M. F. Hawthorne, *Inorg. Chem.*, **13**, 1397 (1974).
(24) J. Lewis, *Pure Appl. Chem.*, **10**, 11 (1965).
(25) B. R. Penfold, *Perspect. Struct. Chem.*, **2**, 71 (1968).
(26) Typical values are in the range of 1.7–1.9 Å, but bonded B–B distances of 2.0 Å or larger have been observed in "normal" $2n + 2$ electron closed polyhedral metallocarboranes, e.g., in the tricapped trigonal prismatic species $(\eta^5\text{-}C_5H_5)CoCB_7H_8^{-}$ [27] and 1,7,5,6-$(\eta^5\text{-}C_5H_5)_2Co_2C_2B_5H_7$.[21]
(27) K. P. Callahan, C. E. Strouse, A. L. Sims, and M. F. Hawthorne, *Inorg. Chem.*, **13**, 1393 (1974).
(28) **Note Added in Proof.** The cobalt–boron cluster $(\eta^5\text{-}C_5H_5)_4Co_4B_4H_4$ recently reported from our laboratory (V. R. Miller and R. N. Grimes, *J. Am. Chem. Soc.*, **98**, 1600 (1976)) is an electron-hyperdeficient ($2n$-electron) framework for which a capped pentagonal bipyramidal structure is possible in the solid state. However, NMR evidence strongly favors D_{2d} dodecahedral geometry in solution.

Chemistry of Dicarbonyl η^5-Cyclopentadienyl-η^1-allyl- and -η^2-olefiniron Complexes. Preparation and Cycloaddition Reactions

A. Cutler, D. Ehntholt, W. P. Giering, P. Lennon, S. Raghu, A. Rosan, M. Rosenblum,* J. Tancrede, and D. Wells

Contribution from the Department of Chemistry, Brandeis University, Waltham, Massachusetts 02154.

Received October 9, 1975

Abstract: A number of η^1-allylmetal complexes of iron, tungsten, molybdenum, cobalt, and chromium enter in (3 + 2) cycloaddition reactions with tetracyanoethylene (TCNE). Of these η^5-$C_5H_5Fe(CO)_2$-η^1-allyl **3a** is the most reactive. This substance and its analogues **7** and **8** may be prepared by metalation of allyl halides or tosylates with η^5-$C_5H_5Fe(CO)_2Na$ or by deprotonation of η^5-$C_5H_5Fe(CO)_2$(olefin) cations **9** and **10**. The scope of the metalation reaction is considered and evidence is provided for rapid equilibration in these complexes. Several general methods are available for the preparation of these iron(olefin) cations. These include olefin exchange with η^5-$C_5H_5Fe(CO)_2$(isobutylene)$^+$ or epoxide deoxygenation with η^5-$C_5H_5Fe(CO)_2Na$. The deprotonation of η^5-$C_5H_5Fe(CO)_2$(olefin) cations is simply achieved by treatment with tertiary amines and is shown to involve preferential loss of a proton trans to the iron–olefin bond. Acyclic and cyclic allyl complexes are readily converted to their TCNE adducts, or in the presence of isocyanates to butyrolactams. These cycloaddition reactions are shown to occur stereospecifically by a suprafacial addition of the electrophile trans to the η^5-$C_5H_5Fe(CO)_2$ group. An analysis of the NMR spectra of several of these iron complexes, both neutral and cationic, indicates a significant diamagnetic anisotropy for the η^5-$C_5H_5Fe(CO)_2$ group in which regions of space close to the fivefold axis of the C_5H_5 ring are relatively shielding. A number of processes are shown to compete with closure of the zwitterion formed as an intermediate in cycloaddition reactions. These include proton transfer, intramolecular decomposition of the zwitterion, and displacement of the anionic terminus at the metal center. Acceptor components such as dicyanodichloroquinone, methylene malonate, and sulfene are also shown to enter into cycloaddition reactions with η^5-$C_5H_5Fe(CO)_2$-η^1-allyl complexes.

Recently we suggested that formation of chain inverted metal allyl sulfones from the reaction of sulfur dioxide with η^1-allyl transition metal complexes was best interpreted in terms of the two-step process depicted in eq 1,[1] rather than by a concerted mechanism.[2]

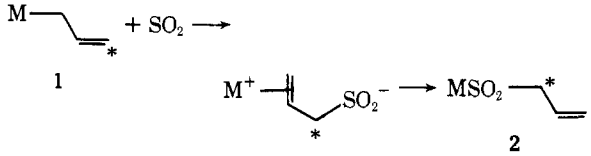

1 2 (1)

At that time we were led to consider the possibility that dipolar ions analogous to **2** might alternatively collapse through addition of the nucleophile to the activated olefin rather than by ligand displacement (eq 2).

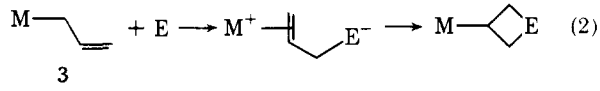

3 (2)

Such metal assisted cycloadditions have since been shown to be very general for a number of electrophiles and η^1-allylmetal complexes.[1,3] A closely related mechanism was also